IOSR Journal of Applied Chemistry (IOSR-JAC)
e-ISSN: 2278-5736.Volume 15, Issue 5 Ser. I (May 2022), PP 13-22
www.iosrjournals.org

Synthesis and crystal structure of 4-chloro-[2-(4,5-diphenyl-1H-imidazol-2-yl)-6-(4,5-diphenyl-1H-imidazol-3-ium-2-yl)]phenol nitrate

Alioune Fall[a], Bédié Mbow[a], Farba Bouyagui Tamboura[b], Mohamed Gaye[a*]
[a]*Department of Chemistry, University Cheikh Anta Diop, Dakar 10700, Senegal*
[b]*Department of Chemistry, UFR SATIC, University Alioune DIOP, Bambey 21400, Senegal*

Abstract: *The symmetrical compound 4-chloro-2,6-bis(4,5-diphenyl-1H-imidazol-2-yl)phenol (**I**) was synthetized from the rection of benzil with 2,6-diformyl-4-chlorophenol in presence of ammonium acetate and glacial acetic acid. After isolation, one arm of the compound was monoprotonated with nitric acid to yield the nitrate salt (**II**). The compounds were characterized by physico-chemical analyses, elemental analysis and FTIR spectroscopy. The structure of the compound **II** was determined by single-crystal X-ray diffraction study. The nitrate salt crystallizes in the monoclinic space group $P2_1/c$ with the following unit cell parameters: a = 14.682 (5) Å, b = 14.514 (5) Å, c = 18.460 (5) Å, β = 128.210 (5)°, V = 3090.9 (17) $Å^3$, Z = 4, R_1 = 0.071 and wR_2 = 0.203. The dihedral angle between the mean planes of the imidazol rings is 48.91 (2)°. The crystal packing of compound (**II**) is stabilized by intramolecular N(imidazol)–H···O(phenol), O(phenol)–H···N(imidazol) and intermolecular N(imidazol)–H···O(nitrate), C(phenyl)–H···O(nitrate) and C(phenyl)–H···Cl hydrogen bonds, leading to the formation of three dimensional network.*

Keywords*: Benzil, 2,6-diformyl-4-chlorophenol, Ammonium acetate, Spectroscopies, X-ray.*

Date of Submission: 28-04-2022 Date of Acceptance: 10-05-2022

I. Introduction

Compounds containing one or more imidazole moieties constitute an important class of synthetic [1,2] or natural heterocyclic molecules [3,4]. They have interesting biological properties. The scientific literature contains examples of this type of molecules with pharmacological properties and playing an important role in biochemical processes. Biotin [5], histamine [6] and histidine [7] are examples of imidazole derivatives playing a central role in biochemistry. The important role that imidazole derivatives play in organic synthesis is well developed in the literature. Indeed, many compounds with an imidazole moiety have analgesic [8,9], antibacterial [10,11], antifungal [12,13], antiepileptic [14], antiparasitic [15,16] or antitumor [17,18] properties. Imidazole derivatives also provide ligands capable of playing a fundamental role in coordination chemistry. Many complexes derived from ligands containing an imidazole moiety yield important physical properties. Indeed, these multidentate ligands give complexes with magnetic [19,20], electrochemical [21,22], optical [23,24], luminescent [25,26] and anticancer [27,28] properties. Because of this wide application of compounds containing an imidazole moiety, these molecules have received particular attention from researchers. Their synthesis is often an art for the chemist despite the high cost of starting materials. Since Debus [29] reported the reaction between ammonia and glyoxal, this pathway is used for the synthesis of compounds having an imidazole moiety. Based on these facts, many authors have synthesized aryl imidazole compounds with very important biological properties [30-33]. Herein, we report the synthesis of 4-chloro-2,6-bis(4,5-diphenyl-1H-imidazol-2-yl)phenol (**I**) and the crystal structure of its nitrate salt (**II**).

II. Experimental

2.1. Starting materials and instrumentations

Benzil, 4-chlorophenol, manganese dioxide, and ammonium acetate were purchased from Sigma-Aldrich and used as received without further purification. All solvents used were of reagent grade. Melting points were determined on a Büchi 570 melting-point apparatus and were uncorrected. Elemental analyses of C, H and N were recorded on a VxRio EL Instrument. Infrared spectra were obtained on an FTIR Spectrum Two

* Corresponding author : mohamedl.gaye@ucad.edu.sn

of Perkin Elmer spectrometer in the 4000-400 cm^{-1} region. The ^{1}H and ^{13}C NMR spectra were recorded in DMSO-d_6 on a BRUKER 500 MHz spectrometer at room temperature using TMS as an internal reference.

2.2. Synthesis of 2,6-Diformyl-4-chlorophenol

2,6-Diformyl-4-chlorophenol was prepared, improving the method described in the literature [34] by crystallizing the compound in n-hexane. Yield 66 %. M.p, = 131-133 °C. Anal. Calc. for $C_8H_5ClO_3$: C, 52.06; H, 2.73; Cl, 19.21 %. Found: C, 52.01; H, 2.713; Cl, 19.19 %. ^{1}H NMR (ppm) 2.84 (3H, s, CH3) ; 7.74 (2H, s, aromatic) ; 10.15 (2H, s, CHO). FTIR (cm^{-1}) 2882 (CH formyl), 1680 (C=O), 125 (C-O).

2.3. Synthesis of 4-chloro-2,6-bis(4,5-diphenyl-1*H*-imidazol-2-yl)phenol (I)

8 mmol of 2,6-diformyl-4-chlorophenol (1.4766 g) were introduced into a 250 mL flask and 16 mmol of benzil (3.362 g) and 128 mmol (9.862 g) of ammonium acetate were added. 30 mL of glacial acetic acid were poured over the above mixture. The mixture was reflux for two hours than a red color was developed. After two hours under reflux, an abundant yellow precipitate appears. 50 mL of distilled water was added to the suspension to complete the precipitation before filtering under vacuum. The precipitate is taken up in dichloromethane and the solution obtained is dried over anhydrous magnesium sulphate. After evaporation of the dichloromethane, a pasty product of reddish color is obtained which is subjected to slow drying. Yield 93.1 %. Anal. Calc. for $C_{36}H_{25}ClN_4O$: C, 76.52; H, 4.46; Cl, 6.27; N, 9.92 %. Found: C, 76.50; H, 4.44; Cl, 6.24; N, 9.89 %. IR (ν, cm^{-1}) : 3389 (O—H), 3160 (N—H), 2924 (C—H), 1583 (C=N), [1545–1420] (C_{Ar}=C_{Ar}), 1280 (C—N).

2.4. Synthesis of the nitrate salt of 4-chloro-[2-(4,5-diphenyl-1*H*-imidazol-2-yl)-6-(4,5-diphenyl-1*H*-imidazol-3-ium-2-yl)]phenol nitrate (II)

To a 5 mL absolute ethanol solution of 4-chloro-2,6-bis(4,5-diphenyl-1H-imidazol-2-yl)phenol (1 mmol), 1 mmol (63 µL) of concentrated nitric acid (70%) was added. The solution was stirred for 30 minutes and left to slow evaporation. One week later, crystals suitable for X-ray diffraction were isolated. Anal. Calc. for $C_{36}H_{26}ClN_5O_4$: C, 68.84; H, 4.17; Cl, 5.64; N, 11.15 %. Found: C, 68.82; H, 4.14; Cl, 5.62; N, 11.12 %. IR (ν, cm^{-1}) : 3385 (O—H), 3162 (N—H), 2924 (C—H), 1580 (C=N), [1541–1422] (C_{Ar}=C_{Ar}), 1380 (NO_3^-), 1282 (C—N).

2.5. Crystal Structure Determination

Crystals suitable for single-crystal X-ray diffraction, of the reported compound, was grown by slow evaporation of EtOH solution of the compound. Details of the crystal structure solution and refinement are given in Table 1. Diffraction data were collected using a Bruker APEX-II CCD diffractometer with graphite monochromatized MoKα radiation (λ =0.71073 Å). All data were corrected for Lorentz and polarization effects. The structure was solved and refined using the Bruker SHELXTL Software Package [35]. All the structures were refined on F^2 by a full-matrix least-squares procedure using anisotropic displacement parameters for all non-hydrogen atoms [36]. H atoms of the NH group was located in the Fourier difference maps and refined without restraints. Other H atoms were geometrically optimized and refined as riding on their carriers with *U*iso(H) = 1.2*U*eq(C)(1.5 for CH_3 groups). Molecular graphics were generated using *ORTEP-3* [37].

Table 1. Crystallographic data and refinement parameters for compound **II**.

Chemical formula	$C_{36}H_{26}ClN_5O_4$
M_r	628.07
Crystal shape/color	Prismatic/yellowish
Crystal size (mm)	0.30 × 0.20 × 0.15
Crystal system, space group	Monoclinic, $P2_1/c$
a (Å)	14.682 (5)
b (Å)	14.514 (5)
c (Å)	18.460 (5)
β (°)	128.210 (5)
V (Å^3)	3090.9 (17)
Z	4

D_{cal} (g cm^{-3})	1.337
Temperature (K)	293
Radiation type	Mo *K*α
μ (mm^{-1})	0.17
Index ranges	-20 ≤ h ≤ 19 ; -18 ≤ k ≤ 20 ; -17 ≤ l ≤ 25
F'(000)	326
θ range (°)	2.5-25
No. of measured reflections	32366
No. of independent reflections	8973
No. of observed [$I > 2\sigma(I)$] reflections	3107
R_{int}	0.110
$R[F^2 > 2\sigma(F^2)]$	0.071
$wR(F^2)$	0.203
Goodness-of-fit (GOF)	0.93
No. of parameters	515
No. of restraints	0
$\Delta\rho_{max}$, $\Delta\rho_{min}$ (e Å^{-3})	0.24, -0.32

III. Result and discussion

3.1. General study

The compound, 4-chloro-2,6-bis(4,5-diphenyl-1*H*-imidazol-2-yl)phenol (**I**), is obtained by the reaction between benzil, 2,6-diformyl-4-chlorophenol and in 2:1 ratio with a large excess of ammonium acetate in acetic acid medium, under reflux (Scheme 1). Elemental analysis is in accordance with the proposed formula $C_{36}H_{25}ClN_4O$. Upon protonation, a nitrate salt (**II**) is obtained with a proposed formula of $C_{36}H_{26}ClN_5O_4$ which agree with the elemental analyses. The FT-IR spectra of the compounds are recorded and analyzed. The two spectra are quite similar with an additional sharp band at 1380 cm^{-1} for **II**. This band is characteristic of a free nitrate group. The main bands appearing in the two spectra are in the ranges [3490-3480 cm^{-1}], [3165-3160 cm^{-1}], [1585-1580 cm^{-1}], [1545-1540 cm^{-1}] and [1285-1280 cm^{-1}]. These bands are, respectively assigned to ν_{O-H}, ν_{N-H}, $\nu_{C=N,}$ $\nu_{C_{Ar}=C_{Ar}}$, and ν_{C-N}. These bands confirm the presence of the phenolic group and the imidazole ring. The lowering of the band $\nu_{C=N}$ at *ca.* 1582 cm^{-1} is due to the strong conjugation with aromatic systems [38].

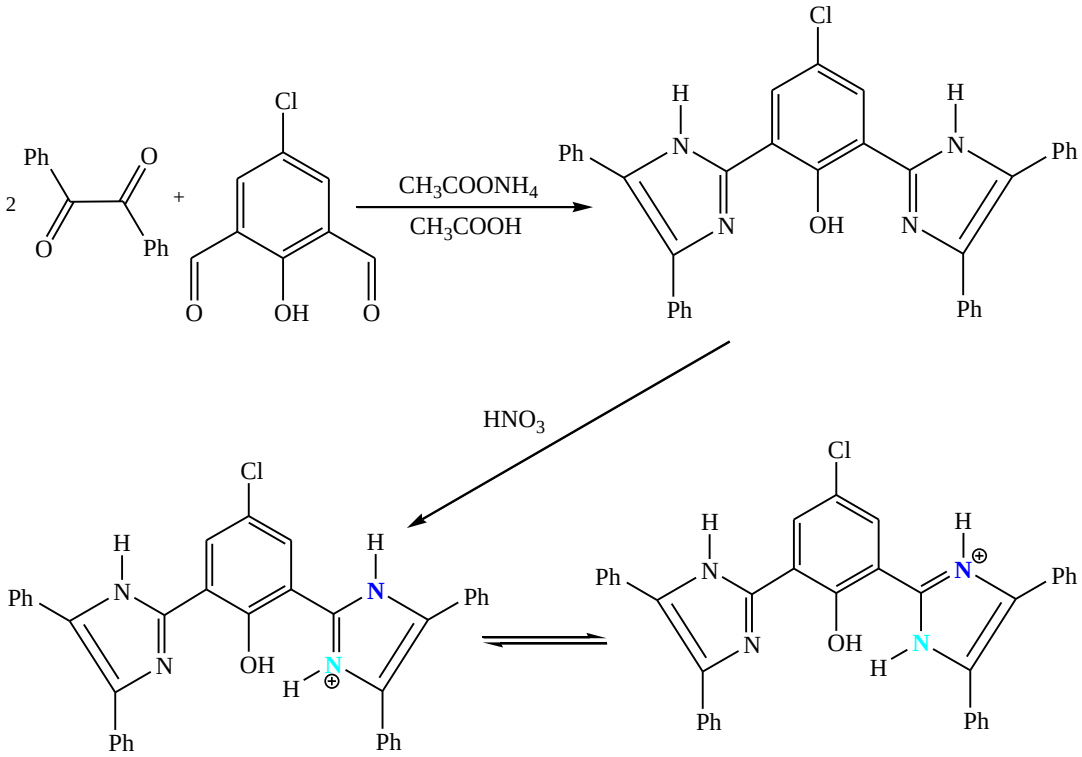

Scheme 1. Synthetic scheme of the compounds and the two superposed resonance structures.

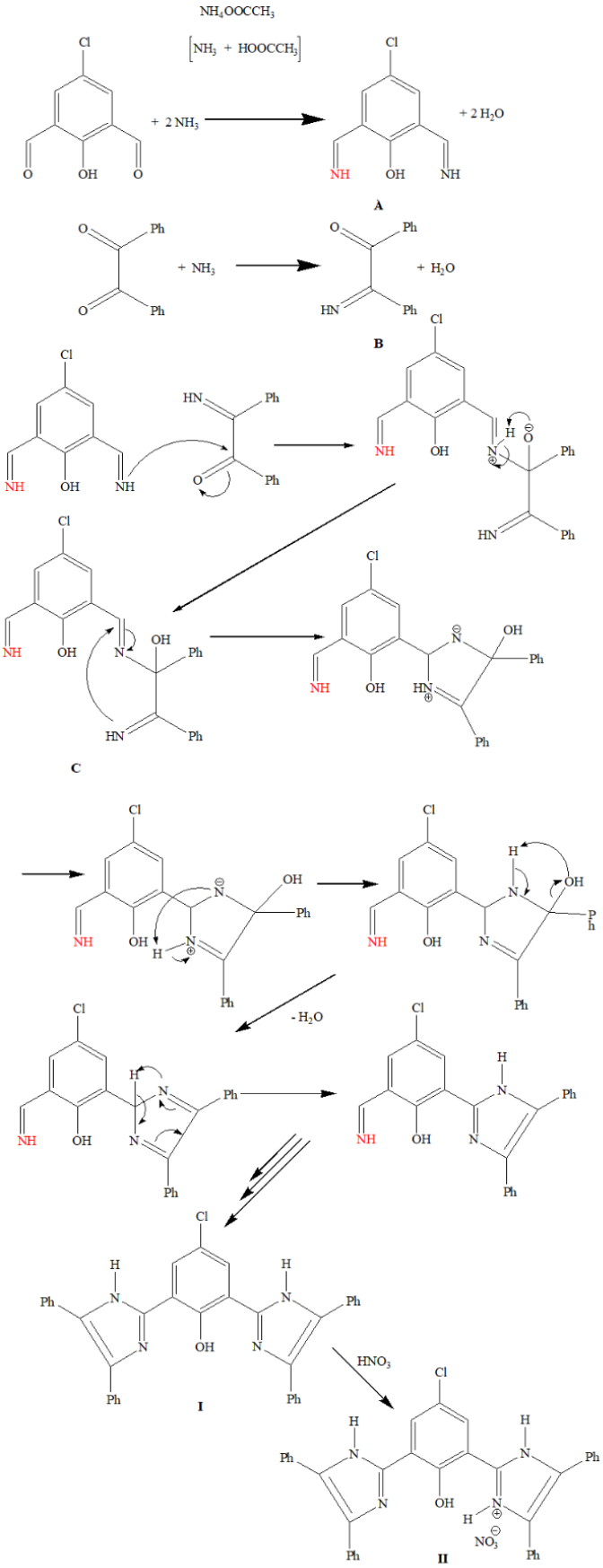

Scheme 2. Proposed mechanism.

3.2. Proposed mechanism

As shown in Scheme 2, the in situ-generated ammonia by ammonium acetate performs a nucleophilic attack on the two carbonyl moieties of the aldehyde 2,6-diformyl-4-chlorophenol which is more reactive and one of the carbonyl functions of the benzil ketone, which is less reactive, resulting in the formation of the imines **A** and **B**. The azomethine of **A** performs a nucleophilic attack on the atom carbon of the remaining carbonyl of **B**, leading to the formation of the intermediate **C**. The terminal imine function of intermediate **C** performs an internal nucleophilic attack through the azomethine on the carbon atom of the internal imine function, followed by a loss of one water molecule, resulting in a cyclisation reaction. Thus, imidazole rings are formed yielding the final product **I**.

3.3. Crystal Structure

The compound (**II**) crystallizes in a solution of ethanol left for slow evaporation. The crystallographic data and the selected bonds lengths and angles values are recorded in Table 1 and Table 2, respectively. The *ORTEP* diagram is shown in Figure 1. The compound crystallizes in the monoclinic system with a space group $P2_1c$.

The molecule consists of one imidazole ring substituted at the 2-, 4-, 5-positions with benzene rings and one imidazol-3-ium moiety substituted at the 2-, 4-, 5-positions with benzene rings. The phenyl substituent which carries a hydroxy at the 1-position and a chloride atom at the 4-position, acts as bridge between the imidazole and the imidazol-3-ium rings and is linked to the two moieties at their 2-positions, respectively. The imidazole and the imidazol-3-ium rings form dihedral angles of 7.10 (2) and 43.52 (2)° with the above benzene ring, indicating a twist in the molecule. The benzene rings C9-C14 and C16-C21 at the 4- and 5-positions of the imidazole ring subtend dihedral angle of 30.49 (2)° and 35.08 (1) respectively and form a dihedral angle of 54.01 (1)° between them. The benzene rings C24-C29 and C31-C36 at the 4- and 5-positions of the imidazol-3-ium ring subtend dihedral angle of 61.90 (1)° and 53.60 (1)° respectively and form a dihedral angle of 28.60 (2)° between them. The imidazole and the imidazol-3-ium rings are quite planar with respective rms of 0.0086 Å and 0.0054 Å. The H-hydroxy atom is quite-in-plane of the phenolic group as shown by the torsion angles C2—C1—O1—H1 (178.39 (3)°) and C6—C1—O1—H1 (-0.44 (3)°).

The bond lengths C7—N3 and C7—N4 have different values [C7—N3 = 1.339 (3) Å] and [C7—N4 = 1.318 (4) Å] in the imidazole ring, but the distances values of the equivalent bonds in imidazol-3-ium rings are quite identical within standard uncertainties [C22—N2 = 1.323 (3) Å] and [C22—N1 = 1.327 (3) Å]. These bond lengths are comparable to those reported for similar compounds [39,40]. In fact, upon protonation the structure of the resulting imidazole-3-ium can be described as a superposition of two resonance structures as shown in Scheme 1.

In the imidazole ring, the C7—N1 and C8—C15 are formally double bond character, while the other ring bonds are formally simple character (Table 2). In the imidazole-3-ium ring C23—C30 is double bond character, while C22—N1 and C22—N2 bond lengths values are slightly superior to the typical double bond value, but inferior to the typical simple bond value (Table 2). This fact is due to the superposition of two resonance structures (Scheme 1). The O—N—O angles values of 119.5 (3)°, 122.8 (3)° and 117.6 (3)° with sum of 360°, differ from the ideal value of 120° and reflect a non-perfect trigonal-planar geometry. The N—O bond distances of 1.189 (3) Å [N—O2], 1.233 (3) [N—O3] Å and 1.248 (3) [N—O4] Å are comparable to those reported for the compound 1-{(*Z*)-1-(2,4-Dichlorophenyl)-1-[2-(4-methylphenoxy)ethoxy]prop-1-en-2-yl}-1H-imidazol-3-ium nitrate [41] and indicate a π delocalization over the two oxygen atom O3 and O4.

The crystal packing of compound (**II**) is stabilized by intramolecular O(phenol)–H···N(imidazole) and N(imidazol)–H···O(phenol), and intermolecular N(imidazol)–H···ONO_2, C(phenyl)–H···ONO_2 and C(phenyl)–H···Cl hydrogen bonds. Intramolecular hydrogen bonds, N1(imidazol)–H01···O1(phenol) and O1(phenol)–H1···N4(imidazol, which close in *S*(6) ring are observed. Intermolecular N1(imidazol)–H01···O4$^{i}NO_2$ (i : -1+x, 1/2-y,-1/2+z), N2(imidazol)–H02···O3$^{ii}NO_2$ (ii : -1+x, y, z), N3(imidazol)–H03···O4$^{iii}NO_2$ (iii : 1-x,-1/2+y, 1/2-z), C5(Phenyl)–H5···O3$^{iii}NO_2$, C26(Phenyl)–H26···Cl^{iv} (iv : x, 1/2-y,-1/2+z) and C32(Phenyl)–H32··· O2$^{v}NO_2$ (v : 1-x, 1/2+y,1/2-z) lead to the formation of a three dimensional network (Figure 2, Table 3).

Table-2. Selected geometric parameters (Å, °) of compound (**II**).

O1—C1	1.337 (3)	C7—N3	1.339 (3)
N1—C22	1.323 (3)	C7—C6	1.467 (4)
N1—C23	1.371 (4)	N3—C8	1.387 (4)
N2—C22	1.327 (3)	C5—C4	1.376 (4)

N2—C30	1.387 (3)	C5—C6	1.386 (4)
C2—C22	1.461 (4)	C23—C24	1.471 (4)
C3—C4	1.381 (4)	C30—C31	1.473 (4)
N4—C7	1.318 (4)	C8—C9	1.469 (4)
C15—C16	1.474 (4)	N5—O3	1.233 (3)
N5—O2	1.189 (3)	N5—O4	1.248 (3)
N1—C22—C2	124.9 (2)	N3—C7—C6	127.2 (3)
N2—C22—C2	128.9 (2)	N1—C23—C24	121.3 (2)
N4—C7—C6	122.1 (3)	N4—C15—C16	119.6 (3)

Table-3. Hydrogen-bond geometry (Å, °).

D—H···A	*D*—H	H···*A*	*D*···*A*	*D*—H···*A*
O1—H1···N4	0.77(5)	1.83(4)	2.545(4)	154(4)
N1—H01···O1	0.73(3)	2.51(3)	2.774(4)	104(2)
N1—H01···O4^{i}	0.73(3)	2.13(3)	2.832(4)	160(3)
N2—H02···O3^{ii}	0.78(3)	1.99(3)	2.749(4)	163(3)
N3—H03···O4^{iii}	0.84(3)	2.19(3)	3.032(4)	176(3)
C5—H5···O3^{iii}	0.86(3)	2.53(3)	3.298(4)	150(2)
C26—H26···Cl1^{iv}	1.06(7)	2.79(5)	3.623(6)	136(4)
C32—H32···O2^{v}	0.91(4)	2.58(3)	3.306(7)	138(2)

Symmetry codes : i = -1+x, 1/2-y,-1/2+z; ii = -1+x, y, z; iii = 1-x,-1/2+y, 1/2-z; iv = x, 1/2-y,-1/2+z; v = 1-x, 1/2+y,1/2-z.

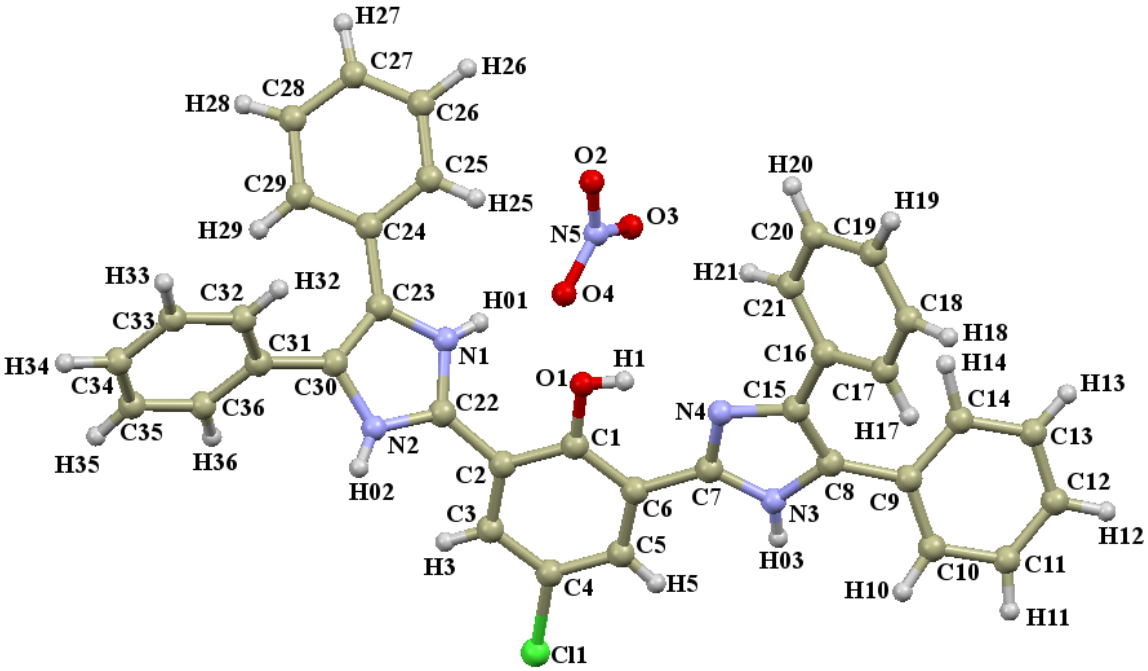

Figure 1. Crystal structure of the compound **II**.

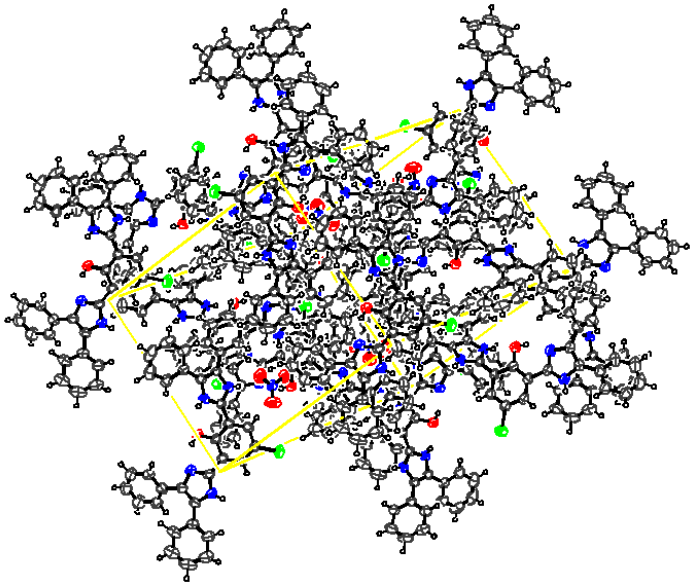

Figure 2. The packing of the compound in the crystal structure

IV. Conclusion

The compound (**II**) namely, 4-chloro-[2-(4,5-diphenyl-1*H*-imidazol-2-yl)-6-(4,5-diphenyl-1*H*-imidazol-3-ium-2-yl)]phenol nitrate was prepared by protonation of compound (**I**) 4-chloro-2,6-bis(4,5-diphenyl-1*H*-imidazol-2-yl)phenol which was successfully prepared by multi-steps reaction of 2,6-diformyl-4-chlorophenol, benzil and ammonium acetate. The structure of compounds (**I**) and (**II**) was confirmed by elemental analysis and FT-IR spectroscopic. The mechanism of the formation of compound (**I**) is depicted. The molecular structure compound (**II**) was also determined by and X-ray diffraction technique.

V. Supporting information

CCDC-2169226 contains the supplementary crystallographic data for this paper. These data can be obtained free of charge via http://www.ccdc.cam.ac.uk/conts/retrieving.html, or from the Cambridge Crystallographic Data Centre, 12 Union Road, Cambridge CB2 1EZ, UK; fax: (+44)-1223-336-033; e-mail: deposit@ccdc.cam.ac.uk (or www:http://www.ccdc.cam.ac.uk).

References

[1]. Lefebvre C.; Fortier L.; Hoffmann N. Photochemical rearrangements in heterocyclic chemistry. European Journal of Organic Chemistry. **2020**, 2020(10), 1393–1404. https://doi.org/10.1002/ejoc.201901190.

[2]. Vargová, D.; Némethová, I.; Šebesta, R. Asymmetric copper-catalyzed conjugate additions of organometallic reagents in the syntheses of natural compounds and pharmaceuticals. Organic & Biomolecular Chemistry. **2020**, 18(20), 3780–3796. https://doi.org/10.1039/D0OB00278J.

[3]. Rocha, J.A.; Andrade, I.M.; Véras, L.M.C.; Quelemes, P.V.; Lima, D.F.; Soares, M.J.S.; Pinto, P.L.S.; Mayo, S.J.; Ivanova, G.; Rangel, M.; Correia, M.; Mafud, A.C.; Mascarenhas, Y.P.; Delerue-Matos, C.; de Moraes, J.; Eaton, P.; Leite, J.R.S.A. Anthelmintic, antibacterial and cytotoxicity activity of imidazole alkaloids from pilocarpus microphyllus leaves. Phytotherapy Research. **2017**, 31(4), 624–630. https://doi.org/10.1002/ptr.5771.

[4]. Babizhayev, M.A.; Courbebaisse, Y.; Nicolay, J.-F.; Semiletov, Y.A. Design and biological activity of imidazole-containing peptidomimetics with a broad-spectrum antioxidant activity. Letters in Peptide Science. **1998**, 5(2), 163–169. https://doi.org/10.1007/BF02443462.

[5]. Tong, L. Structure and function of biotin-dependent carboxylases. Cellular and Molecular Life Sciences. **2013**, 70(5), 863–891. https://doi.org/10.1007/s00018-012-1096-0.

[6]. Nieto-Alamilla, G.; Márquez-Gómez, R.; García-Gálvez, A.-M.; Morales-Figueroa, G.-E.; Arias-Montaño, J.-A. The histamine H3 receptor: structure, pharmacology, and function. Molecular Pharmacology. **2016**, 90(5), 649–673. https://doi.org/10.1124/mol.116.104752.

[7]. Mihailescu, M.; Sorci, M.; Seckute, J.; Silin, V.I.; Hammer, J.; Perrin, B.S.; Hernandez, J.I.; Smajic, N.; Shrestha, A.; Bogardus, K.A.; Greenwood, A.I.; Fu, R.; Blazyk, J.; Pastor, R.W.; Nicholson, L.K.; Belfort, G.; Cotten, M.L. Structure and function in antimicrobial piscidins: histidine position, directionality of membrane insertion, and ph-dependent permeabilization. Journal of the American Chemical Society. **2019**, 141(25), 9837–9853. https://doi.org/10.1021/jacs.9b00440.

[8]. Uçucu, Ü.; Karaburun, N.G.; Işikdağ, İ. Synthesis and analgesic activity of some 1-benzyl-2-substituted-4,5-diphenyl-1h-imidazole derivatives. Il Farmaco. **2001**, 56(4), 285–290. https://doi.org/10.1016/S0014-827X(01)01076-X.

[9]. Caliendo, G.; Cirino, G.; Greco, G.; Novellino, E.; Perissutti, E.; Pinto, A.; Santagada, V.; Sorrentino, L. Synthesis and anti-inflammatory analgesic profile of 1-methyl-2-(4-x-benzoyl) imidazole-5-carboxylic acids. European Journal of Medicinal Chemistry. **1995**, 30(4), 315–320. https://doi.org/10.1016/0223-5234(96)88239-0.

[10]. Günsel, A.; Taslimi, P.; Atmaca, G.Y.; Bilgiçli, A.T.; Pişkin, H.; Ceylan, Y.; Erdoğmuş, A.; Yarasir, M.N.; Gülçin, İ. Novel potential metabolic enzymes inhibitor, photosensitizer and antibacterial agents based on water-soluble phthalocyanine bearing imidazole derivative. Journal of Molecular Structure. **2021**, 1237, 130402. https://doi.org/10.1016/j.molstruc.2021.130402.

[11]. Bulut, O.; Oktem, H.A.; Yilmaz, M.D. A highly substituted and fluorescent aromatic-fused imidazole derivative that shows enhanced antibacterial activity against methicillin-resistant *staphylococcus aureus* (MRSA). Journal of Hazardous Materials. **2020**, 399, 122902. https://doi.org/10.1016/j.jhazmat.2020.122902.

[12]. Khodja, I.A.; Boulebd, H.; Bensouici, C.; Belfaitah, A. Design, synthesis, biological evaluation, molecular docking, DFT calculations and in silico ADME analysis of(benz)imidazole-hydrazone derivatives as promising antioxidant, antifungal, and anti-acetylcholinesterase agents. Journal of Molecular Structure. **2020**, 1218, 128527.https://doi.org/10.1016/j.molstruc.2020.128527.

[13]. Zhao, S.; Zhao, L.; Zhang, X.; Wei, P.; Wu, M.; Su, X.; Sun, B.; Zhao, D.; Cheng, M. Design, synthesis and evaluation of biphenyl imidazole analogues as potent antifungal agents. Bioorganic & Medicinal Chemistry Letters. **2019**, 29(17), 2448–2451. https://doi.org/10.1016/j.bmcl.2019.07.037.

[14]. Ganguly, S.; Mishra, R. Comparative molecular similarity indices analysis of 1-(naphthylalky1)–1*H*-imidazole analogs with antiepileptic activity. Journal of Young Pharmacists. **2010**, 2(4), 388–393. https://doi.org/10.4103/0975-1483.71635.

[15]. Hernández-Núñez, E.; Tlahuext, H.; Moo-Puc, R.; Torres-Gómez, H.; Reyes-Martínez, R.; Cedillo-Rivera, R.; Nava-Zuazo, C.; Navarrete-Vazquez, G. Synthesis and in *vitro* trichomonicidal, giardicidal and amebicidal activity of *N*-acetamide(sulfonamide)-2-methyl-4-nitro-1*H*-imidazoles. European Journal of Medicinal Chemistry. **2009**, 44(7), 2975–2984. https://doi.org/10.1016/j.ejmech.2009.01.005.

[16]. Adeyemi, O.S.; Eseola, A.O.; Plass, W.; Kato, K.; Otuechere, C.A.; Awakan, O.J.; Atolani, O.; Otohinoyi, D.A.; Elebiyo, T.C.; Evbuomwan, I.O. The anti-parasite action of imidazole derivatives likely involves oxidative stress but not HIF-1α signaling. Chemico-Biological Interactions. **2021**, 349, 109676. https://doi.org/10.1016/j.cbi.2021.109676.

[17]. Hassan, A.Y.; El-Sebaey, S.A.; Deeb, M.A.E.; Elzoghbi, M.S. Potential antiviral and anticancer effect of imidazoles and bridgehead imidazoles generated by HPV-induced cervical carcinomas via reactivating the P53/ PRb pathway and inhibition of CA IX. Journal of Molecular Structure. **2021**, 1230, 129865.https://doi.org/10.1016/j.molstruc.2020.129865.

[18]. Yang, Y.-Q.; Chen, H.; Liu, Q.-S.; Sun, Y.; Gu, W. Synthesis and anticancer evaluation of novel 1*H*-benzo[d]imidazole derivatives of dehydroabietic acid as PI3Kα inhibitors. Bioorganic Chemistry. **2020**, 100, 103845. https://doi.org/10.1016/j.bioorg.2020.103845.

[19]. Tanaka, T.; Sunatsuki, Y.; Suzuki, T. Synthesis and magnetic properties of tetrahedral tetranuclear iron(II) complexes with bis(bidentate)-type Schiff bases containing imidazole groups. Inorganica Chimica Acta. **2020**, 502, 119373. https://doi.org/10.1016/j.ica.2019.119373.

[20]. Godlewska, S.; Jezierska, J.; Baranowska, K.; Augustin, E.; Dołęga, A. Copper(II) complexes with substituted imidazole and chlorido ligands: X-Ray, UV–Vis, magnetic and epr studies and chemotherapeutic potential. Polyhedron. **2013**, 65, 288–297. https://doi.org/10.1016/j.poly.2013.08.039.

[21]. An, Y.; Li, X.-F.; Sun, J.-J.; Tong, S.-F.; Yang, H.; Yang, S.-P.; Dong, L.-H.; Yin, Y.-S. Self-assembly, electrochemistry and magnetic behaviors of cobalt complexes with featuring imidazole–tripodal ligand. Inorganic Chemistry Communications. **2014**, 40, 211–214. https://doi.org/10.1016/j.inoche.2013.12.004.

[22]. Beloglazkina, E.K.; Majouga, A.G.; Mironov, A.V.; Yudina, A.V.; Moiseeva, A.A.; Lebedeva, M.A.; Khlobystov, A.N.; Zyk, N.V. Synthesis, X-ray crystallography and electrochemistry of three novel copper complexes with imidazole-containing hydantoin and thiohydantoins. Polyhedron. **2013**, 63, 15–20. https://doi.org/10.1016/j.poly.2013.07.014.

[23]. Li, T.; Hu, Y. Single crystal structure of cobalt and nickel complexes constructed by imidazole ligand and their polycrystalline thin films for nonlinear optical refraction properties. Journal of Molecular Structure. **2022**, 1260, 132851. https://doi.org/10.1016/j.molstruc.2022.132851.

[24]. Yazdani, A.; Pitchunmony, T.S.; Banevicius, L.; Czorny, S.; Valliant, J.F. Imidazole stabilized [2+1] Re(I)/99mTc(I) complexes as isostructural nuclear and optical probes. Nuclear Medicine and Biology. **2014**, 41(7), 616. https://doi.org/10.1016/j.nucmedbio.2014.05.101.

[25]. Gao, F.; Chen, X.; Zhou, F.; Weng, L.-P.; Guo, L.-T.; Chen, M.; Chao, H.; Ji, L.-N. pH responsive luminescent switches of ruthenium(II) complexes containing two imidazole groups: synthesis, spectroscopy, electrochemistry and theoretical calculations. Inorganica Chimica Acta. **2009**, 362(14), 4960–4966. https://doi.org/10.1016/j.ica.2009.07.034.

[26]. Lu, Y.; Li, X.; Wang, J.; Zhao, F.; Wang, Y.; He, H.; Wu, Y. Synthesis, characterization and DFT studies of luminescent copper(I) complexes containing pyridine-imidazole ligands with tunable π-conjugation system via variation of polyaromatic groups. Journal of Photochemistry and Photobiology A: Chemistry. **2022**, 422, 113566. https://doi.org/10.1016/j.jphotochem.2021.113566.

[27]. Fernández-Pampín, N.; Vaquero, M.; Gil, T.; Espino, G.; Fernández, D.; García, B.; Busto, N. Distinct mechanism of action for antitumoral neutral cyclometalated Pt(II)-complexes bearing antifungal imidazolyl-based drugs. Journal of Inorganic Biochemistry. **2022**, 226, 111663. https://doi.org/10.1016/j.jinorgbio.2021.111663.

[28]. Kaps, L.; Biersack, B.; Müller-Bunz, H.; Mahal, K.; Münzner, J.; Tacke, M.; Mueller, T.; Schobert, R. Gold(I)–NHC complexes of antitumoral diarylimidazoles: structures, cellular uptake routes and anticancer activities. Journal of Inorganic Biochemistry. **2012**, 106(1), 52–58. https://doi.org/10.1016/j.jinorgbio.2011.08.026.

[29]. Debus, H. Ueber die einwirkung des ammoniaks auf glyoxal. Justus Liebigs Annalen der Chemie. **1858**, 107(2), 199–208. https://doi.org/10.1002/jlac.18581070209.

[30]. Oskuei, S.R.; Mirzaei, S.; Jafari-Nik, M.R.; Hadizadeh, F.; Eisvand, F.; Mosaffa, F.; Ghodsi, R. Design, synthesis and biological evaluation of novel imidazole-chalcone derivatives as potential anticancer agents and tubulin polymerization inhibitors. Bioorganic Chemistry. **2021**, 112, 104904. https://doi.org/10.1016/j.bioorg.2021.104904.

[31]. Sethiya, A.; Soni, J.; Sahiba, N.; Teli, P.; Agarwal, D.K.; Agarwal, S. Chapter 2 - biological profile of imidazole-based compounds as anticancer agents.in imidazole-based drug discovery. Agarwal, S., Ed, Heterocyclic Drug Discovery; Elsevier. **2022**, pp 35–131. https://doi.org/10.1016/B978-0-323-85479-5.00005-8.

[32]. Edukondalu, P.; Sireesha, R.; Bandaru, C.M.; Rao, M.V.B.; Kala, P.; Raju, R.R. Design, synthesis and anticancer evaluation of 2-(5-(benzo[d]thiazol-2-yl)-1h-imidazol-1-yl)-5-aryl-1*H*-benzo[d]imidazole derivatives. Chemical Data Collections. **2021**, 35, 100753. https://doi.org/10.1016/j.cdc.2021.100753.

[33]. Yang, X.; Sun, H.; Maddili, S.K.; Li, S.; Yang, R.-G.; Zhou, C.-H. Dihydropyrimidinone imidazoles as unique structural antibacterial agents for drug-resistant gram-negative pathogens. European Journal of Medicinal Chemistry. **2022**, 232, 114188. https://doi.org/10.1016/j.ejmech.2022.114188.

[34]. Taniguchi, S. Oxidation of 2,6-bis(hydroxymethyl)phenols to 2-hydroxyisophthalaldehydes by MnO_2. Bulletin of the Chemical Society of Japan. **1984**, 57(9), 2683–2684. https://doi.org/10.1246/bcsj.57.2683.
[35]. Sheldrick, G.M. *SHELXT* – Integrated space-group and crystal-structure determination. Acta Crystallographica Section A: Foundations and Advances. **2015**, 71(1), 3–8. https://doi.org/10.1107/S2053273314026370.
[36]. Sheldrick, G.M. Crystal structure refinement with *SHELXL*. Acta Crystallographica Section C: Structural Chemistry. **2015**, 71(1), 3–8. https://doi.org/10.1107/S2053229614024218.
[37]. Farrugia, L.J. *WinGX* and *ORTEP* for Windows: an update. Journal of Applied Crystallography. **2012**, 45(4), 849–854. https://doi.org/10.1107/S0021889812029111.
[38]. White, D.M.; Sonnenberg, J. Infrared spectra of arylimidazoles and arylisoimidazoles. Journal of Organic Chemistry. **1964**, 29(7), 1926–1930. https://doi.org/10.1021/jo01030a064.
[39]. Archana, S.D.; Kavitha, C.N.; Yathirajan, H.S.; Foro, S.; Glidewell, C. Two 3-amino-1*H*-pyrazol-2-ium salts containing organic anions, and an orthorhombic polymorph of 3-amino-1*H*-pyrazol-2-ium nitrate. Acta Crystallographica Section E: Crystallographic Communications. **2021**, 77(1), 34–41. https://doi.org/10.1107/S2056989020015959.
[40]. Mohamed, S.K.; Marzouk, A.A.; Albayati, M.R.; Abdelhamid, A.A.; Simpson, J. Crystal structure of 1-[2-(4-chlorophenyl)-4,5-diphenyl-1*H*-imidazol-1-yl]propan-2-ol. Acta Crystallographica Section E: Crystallographic Communications. **2017**, 73(1), 59–62. https://doi.org/10.1107/S2056989016019332.
[41]. Guo, S.; Hu, Y.; Luan, Y.; Wang, L.; Yang, W. 1-(*Z*)-1-(2,4-dichlorophenyl)-1-[2-(4-methylphenoxy)ethoxy]prop-1-en-2-yl-1*H*-imidazol-3-ium nitrate. Acta Crystallographica Section E: Crystallographic Communications. **2013**, 69(1), o27. https://doi.org/10.1107/S1600536812046181.

Alioune Fall, et. al. " Synthesis and crystal structure of 4-chloro-[2-(4,5-diphenyl-1H-imidazol-2-yl)-6-(4,5-diphenyl-1H-imidazol-3-ium-2-yl)]phenol nitrate." *IOSR Journal of Applied Chemistry (IOSR-JAC)*, 15(05), (2022): pp 13-22.